Memoirs of the School of Engineering, Okayama University, Vol. 15-1, November 1980

Factors Affecting Plunge Grinding Force

Toshikatsu NAKAJIMA* and Yoshiyuki UNO*

(Received September 29, 1980)

Synopsis

Grinding force has a close relation to grinding inputs such as grinding wheel, work material, interference condition, grinding speed, grinding fluid and machine condition, and therefore varies widely with grinding inputs. On the other hand, grinding force affects significantly grinding outputs which are efficiency and quality evaluated with surface roughness, accuracy, surface integrity and so on. It is important to make clear the relations between grinding inputs and grinding force in order to control grinding outputs.

In this paper, from the above point of view, the relations between grinding inputs and grinding force are experimentally investigated. It is pointed out that the normal grinding force, the tangential grinding force and its ratio are determined by the product of speed ratio of work speed to wheel speed and setting depth of cut as for interference conditions, and by the product of square of dressing feed and cutting depth of dresser as for dressing conditions. Furthermore as for characteristics of work materials, the normal grinding force has a close relation to the yield stress, and the force ratio is related to the elongation of work material.

Department of Mechanical Engineering

1. Introduction

Grinding phenomenon in which many grains on acting wheel surface interfer with workpiece, takes place under various grinding conditions, and consequently various grinding results are obtained. Grinding conditions are classified into the following six conditions, that is, interference condition, relative speed, cutting edge condition, workpiece condition, atmospheric condition (grinding fluid) and machine condition. On the other hand, grinding results are surface roughness, machining accuracy, residual stress, affected layer and so on. It is ideal to control grinding results by grinding conditions. However, it has been impossible up to the present. Because it has been difficult to analyze the complicated relations between grinding conditions and grinding results. It is very significant to make it clear how grinding conditions affect grinding phenomenon for the final purpose of controlling grinding results by grinding conditions. In grinding phenomenon, grinding force, grinding heat, grinding sound and so on are generated. Therefore these values may be indicators which represent the state of grinding phenomenon. Among these values, grinding force can easily be measured and practical. Grinding force in plunge grinding is devided into two components, the normal force P and the tangential force Q as shown in Fig.1. Furthermore the force ratio ρ of tangential force to normal force indicates the direction of resultant force F and has a close relation to grinding phenomenon. From the above mentioned point of view, this paper describes effects of grinding conditions such as interference condition, cutting edge condition and workpiece condition on the grinding force components and the force ratio.

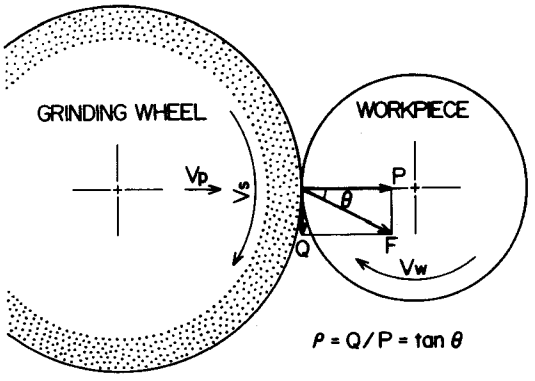

Fig.1 Grinding Force Components P,Q and Force Ratio ρ

2. Experimental procedures

2.1 Grinding Test

Grinding test is carried out in cylindrical plunge grinding.

Grinding force components are measured as shwn in Fig.2 with strain gages which are stuck on the dead center of tail stock. In the experiment, interference condition,cutting edge condition and workpiece condition among grinding inputs are systematically changed. First, as for interference condition, which determines the average undeformed chip shape having complicated relation to wheel speed Vs, work speed Vw, successive cutting edge spacing δ, plunge speed Vp and so on, the speed ratio Kv of work speed Vw to wheel speed Vs and the setting depth of cut Δ are systematically changed while other conditions are kept constant. Next, as for cutting edge condition, which is determined by a grinding wheel specification and a dressing condition, the dressing condition is changed with the grinding wheel WA80L9V. Furthermore, as for workpiece condition, the following five materials are adopted for wide variety of material characteristics. That is, midium carbon steel S45C, cast iron FC20, austenitic stainless steel SUS304, carbon tool steel SK3 and chromium molybdenum steel SCM3 in JIS specifications. Main grinding conditions are shown in Table 1.

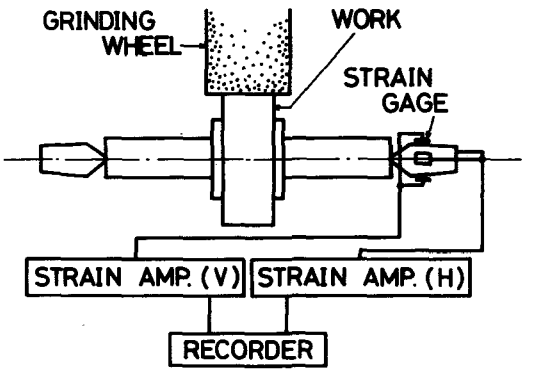

Fig.2 Measuring System of Grinding Force Components

Table 1 Grinding Conditions

Wheel		WA80L9V , φ405mm×50mm
Work	S45C	φ120mm×30mm , Hv=240 kg/mm²
	FC20	φ120mm×30mm , Hv=270 kg/mm²
	SUS304	φ120mm×30mm , Hv=250 kg/mm²
	S K 3	φ120mm×30mm , Hv=720 kg/mm²
	SCM3	φ120mm×30mm , Hv=340 kg/mm²
Dressing Condition		5 μm × 0.05mm/rev. of G.W.
		10 μm × 0.1 mm/rev. of G.W.
		20 μm × 0.2 mm/rev. of G.W.
		40 μm × 0.4 mm/rev. of G.W.
Plunge Speed		Vp = 0.5 ~ 3 μm/sec.
Work Speed		Vw = 11.3 ~ 33.9 m/min.
Wheel Speed		Vs = 2664 m/min.
Speed Ratio		Kv = 0.013 ~ 0.004

2.2 Material Test

In order to obtain basic characteristic values of workpiece materials used for grinding test, tension test and Charpy's impact test are carried out. The sizes of specimens for tension test and Charpy's impact test are shown in Fig.3(a),(b) respectively.

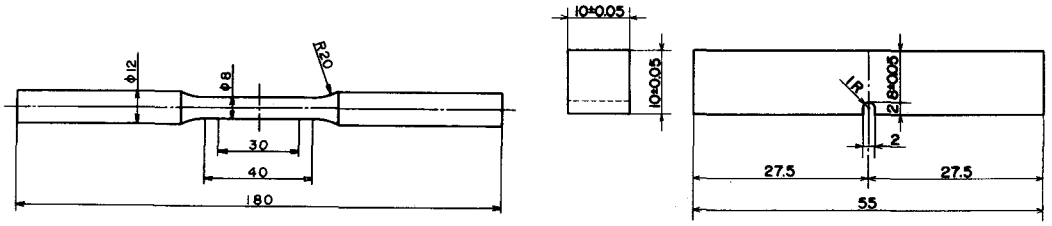

(a) Tension Test (b) Impact Test

Fig.3 Sizes of Specimens

3. Variation of Grinding Force in Grinding Cycle

A plunge grinding cycle is composed of three distinct grinding states, a spark-in, a steady and a spark-out state [1]. Fig.4 shows variations of normal force P, tangential force Q and force ratio ρ in a plunge grinding cycle. In this figure, t_s, t_y, t_f represents spark-in grinding time, steady grinding time and spark-out grinding time respectively. As can be seen in this figure, two grinding force components P and Q increase with grinding time through the spark-in state and become constant in the steady state. Further in the spark-out state, P and Q decrease with grinding time without becoming equal to zero even in the end of effective spark-out grinding. On the other hand, the force ratio ρ is not equal to zero at the beginning of grinding cycle and increases with grinding time

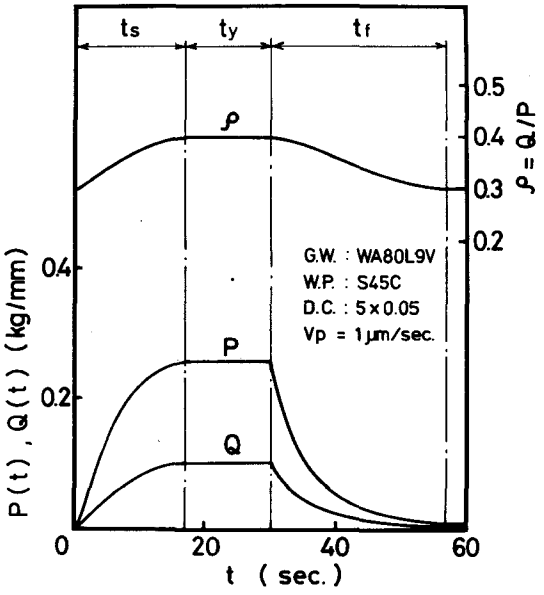

Fig.4 Variations of Normal Force P, Tangential Force Q and Force Ratio ρ in a Plunge Grinding Cycle

through the spark-in state, becomes constant in the steady state and decreases with grinding time through the spark-out state. Finally it becomes the same value as the first value of the spark-in state at the end of effective spark-out grinding. These variation processes have a close relation to accumulation phenomenon in plunge grinding [1]. In plunge grinding, the infeed rate of wheel head Vp is generally selected to be small. In the initial state of such a plunge grinding, essentially no metal removal occurs because the interference depth of wheel is very small and the cutting grains contact only elastically with workpiece [2]. In this stage, Coulomb's friction law can be applied. That is, the force ratio ρ is equal to frictional coefficient μ. Since wheel head advances however at a constant infeed rate and then the interference depth of wheel increases accumulated with grinding time, some metal removal occurs at low rate due to the secondary chip formation process, in which cutting grains plough the workpiece, piling up work material along the sides of the grain path and breaking off a part of the pile up material. At still larger interference depth of wheel, each cutting grain comes to produce chip and thus the size generation rate becomes higher, but the interference depth of wheel increases accumulated with grinding time also in this stage because of smaller rate of size generation than the infeed rate of wheel head. Through this stage, the rate of increase of tangential force Q is larger than that of normal force P because of forces for ploughing and chip removal. So the force ratio ρ increases with grinding time. When the interference depth of wheel becomes much larger than the setting depth of wheel and the size generation rate becomes equal to the effective infeed rate of wheel which is determined as wheel infeed rate minus wheel wear rate, a steady grinding state can be reached. In this state, normal force P and tangential force Q is constant and consequently the force ratio ρ is also constant. Stopping wheel head infeed, the spark-out grinding state takes place with a decrease of accumulated amount in grinding system. In this stage, the process goes by contraries in spark-in state, so two force components decrease with grinding time and the force ratio also decreases. However the accumulated amount in grinding system does not equal to zero even in the end of the effective spark-out grinding [3], therefore two force components become certain constant values respectively caused by elastic contact, and the force ratio ρ is equal to the value at the beginning of a grinding cycle.

4. Effect of Grinding Condition on Grinding Force

4.1 Relation between Interference Condition and Grinding Force

Grinding force is represented as the sum of forces generated by individual cutting grains interfering with workpiece, so the undeformed chip shape is the basis in analyzing grinding force. Interference condition determines directly the undeformed chip shape and this has a complicated relation to the speed ratio Kv, the setting depth of cut Δ, successive cutting edge spacing δ and the like.

Fig.5 shows relations between the setting depth of cut Δ and the normal force Ps, the tangential force Qs in the steady state and the force ratio ρ with the speed ratio Kv. As shown in this figure, grinding force components Ps, Qs and the force ratio ρ increase with larger setting depth of cut Δ along the curve of the constant speed ratio Kv. The increase of force components with setting depth of cut is due to an increase of cross sectional area of undeformed chip shape. Then the increase of force ratio is due to an increase of the ratio of cutting region in which the force ratio is larger than in ploughing or rubbing region as mentioned before. On the other hand, with constant setting depth of cut, grinding force components and the force ratio increase with an increase of speed ratio Kv. The increase of force ratio is due to an increase of interference angle [4] and relative increase of cutting region as compared with ploughing or rubbing region. As mentioned above, the grinding force and the force ratio have a close relation to the undeformed chip shape. However, as seen in Fig.5, the grinding force is not determined by the setting depth of cut Δ, because the manner of

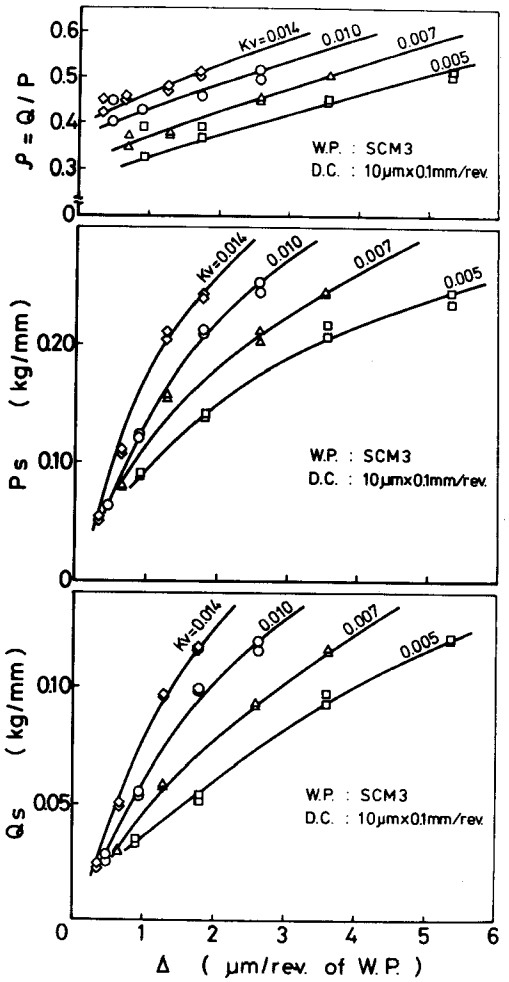

Fig.5 Relations between Setting Depth of Cut Δ and Force Components Ps, Qs and Force Ratio ρ

force variation is different with different speed ratio. It is well known that the grinding force is determined by the product of undeformed chip length Lc and maximum chip thickness tmax [5]. Lc and tmax are however the values which are difficult to measure in practice. Then in this paper, a new parameter is introduced as a result of the following transformation. The undeformed chip length Lc and the maximum chip thickness tmax in Fig.6 are expressed as follows [6],

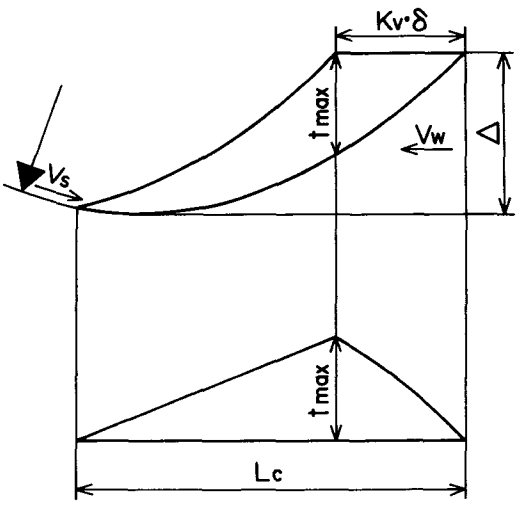

Fig.6 Undeformed Chip Shape

$$Lc = \{2\alpha_s \cdot R_s(1+K_v)+K_v \cdot \delta\}/2 \quad (1)$$

$$tmax = (1+K_R)K_v \cdot \delta\{2\alpha_s \cdot R_s(1+K_v)-K_v \cdot \delta\}/2K_R(1+K_v)^2R_s \quad (2)$$

where

R_s : wheel radius

K_R : ratio of workpiece radius to wheel radius

$2\alpha_s$: contact angle of wheel

The product Lc and tmax is transformed as follows;

$$Lc \cdot tmax = 2K_v \cdot \Delta \cdot \delta-(1+K_R)(K_v \cdot \delta)^3/4K_R(1+K_v)^2R_s \quad (3)$$

The second term of right side in Eq.(3) is neglegible small compared with the first one under conventional grinding condition, then Eq.(3) becomes as follows;

$$Lc \cdot tmax = 2K_v \cdot \Delta \cdot \delta \quad (4)$$

Among the parameters of right side of the equation, the successive cutting edge spacing δ is the parameter which represents directly cutting edge condition, therefore in this experiment, the product of speed ratio Kv and setting depth of cut Δ are adopted as a parameter as for interference condition while the successive cutting edge spacing δ is kept constant.

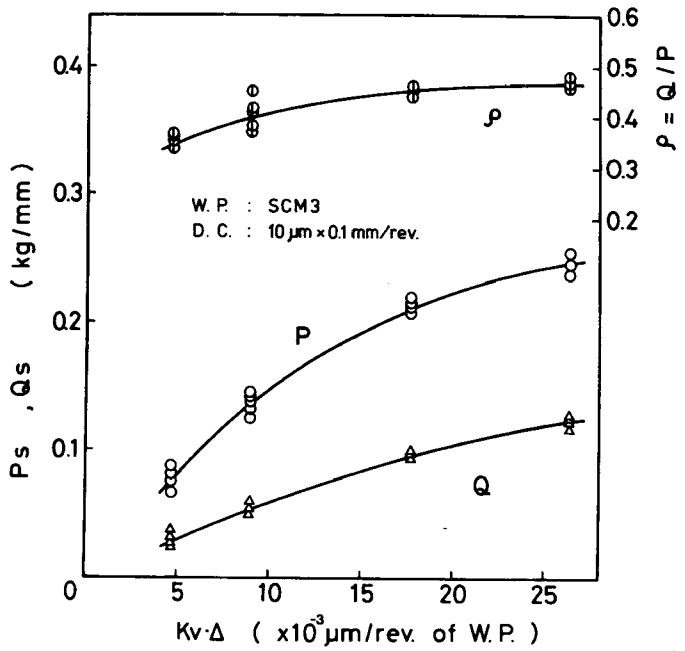

Fig.7 Relations between the Value $K_V \cdot \Delta$ and Force Components Ps, Qs and Force Ratio ρ

Fig.7 shows relations between the value $K_V \cdot \Delta$ and force components Ps, Qs and the force ratio ρ. As can be seen in this figure, force components Ps, Qs and the force ratio ρ are determined by the value Kv·Δ and increase with an increase of the value Kv·Δ.

4.2 Relation between Cutting Edge Condition and Grinding Force

As mentioned in Section 4.1, grinding force is determined by parameter K_V, Δ and δ. Among these parameters, the successive cutting edge spacing δ is concerned with cutting edge condition. The successive cutting edge spacing δ is however the value difficult to measure. Cutting edges on wheel surface are formed by dressing with a single point diamond dresser. In this section, therefore the relation between dressing condition and grinding force is discussed.

Fig.8 shows relations between cutting depth of dresser D_Δ and grinding force components Ps, Qs and the force ratio ρ with parameter of dressing feed per revolution of grinding wheel S. As can be seen in this figure, force components Ps and Qs decrease and then become constant with an increase of cutting depth of dresser D_Δ, while the force ratio ρ increases and then becomes constant. These values vary however

along different curves respectively with different values of dressing feed S.

Fig.9 shows relations between the product of dressing feed S and cutting depth of dresser D_Δ, and force components Ps, Qs and the force ratio ρ. The value $S \cdot D_\Delta$ is concerned with the interference cross sectional area of diamond dresser. As can be seen in this figure, force components Ps and Qs decrease while the force ratio ρ increases with an increase of the value $S \cdot D_\Delta$. However, these values change along different curves with different values of dressing feed S. From Figs.8 and 9, it is shown that D_Δ and/or $S \cdot D_\Delta$ are not factors which determine grinding force and/or force ratio. Then a new parameter, the product of square of dressing feed and cutting depth of dresser $S^2 \cdot D_\Delta$ is introduced.

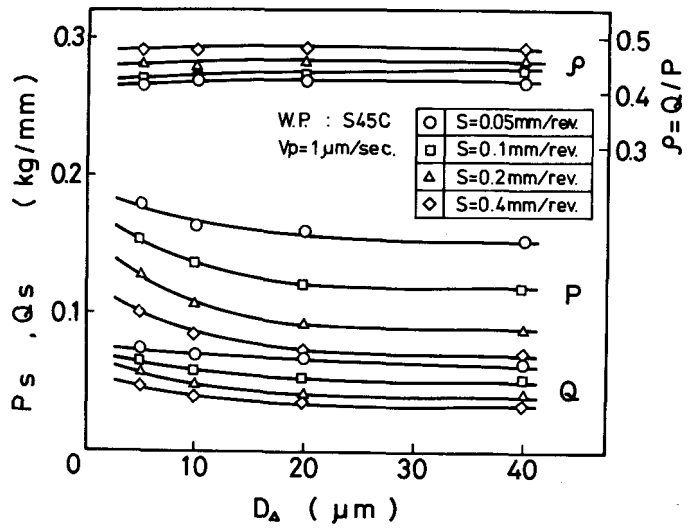

Fig.8 Relations between Cutting Depth of Dresser D_Δ and Force Components Ps, Qs and Force Ratio ρ

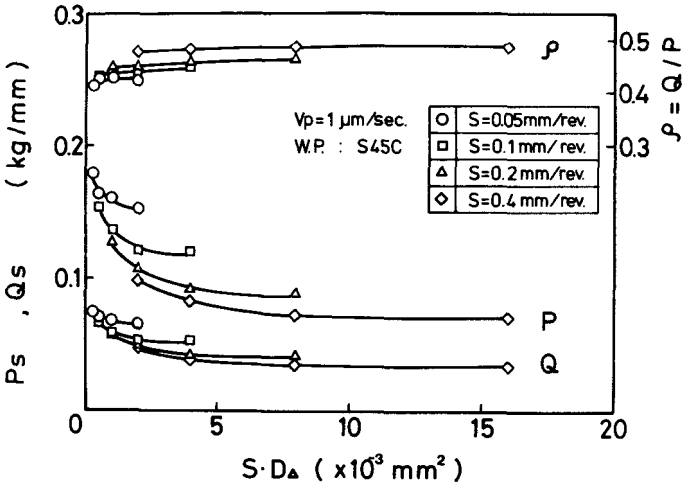

Fig.9 Relations between the Value $S \cdot D_\Delta$ and Force Components Ps, Qs and Force Ratio ρ

Fig.10 shows relations between the value $S^2 \cdot D_\Delta$ and force components Ps, Qs and the force ratio ρ. As shown in this figure, force components Ps, Qs and the force ratio ρ are determined by the value $S^2 \cdot D_\Delta$. The value $S^2 \cdot D_\Delta$ corresponds to the interference volume of diamond dresser on assuming that the shape of dresser is cone. Fine dressing leads to low value of $S^2 \cdot D_\Delta$ and dense distribu-

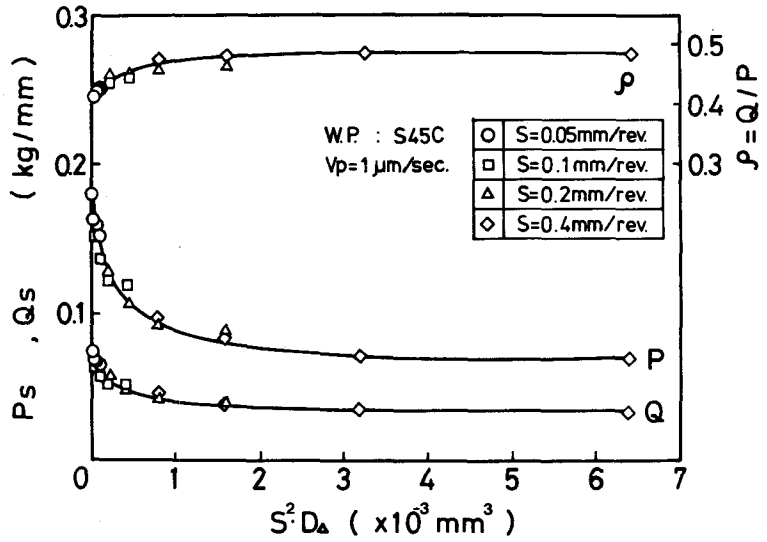

Fig.10 Relations between the Value $S^2 \cdot D_\Delta$ and Force Components Ps, Qs and Force Ratio ρ

tion of cutting edges, on the other hand coarse dressing results in high value of $S^2 \cdot D_\Delta$ and coarse distribution of cutting edges. As a result, force components and the force ratio have a close relation to the interference volume of diamond dresser.

4.3 Relation between Material Condition and Grinding Force

Fig.11 shows relations between the value $K_V \cdot \Delta$ and force components Ps, Qs and the force ratio ρ for five different work materials S45C, FC20, SK3, SCM3 and SUS304 as for interference condition while dressing condition is constant. Only one datum is shown for SUS304 because of impossibility of grinding it under other conditions. As can be seen in this figure, the normal force Ps, the tangential force Qs and the force ratio ρ increase with an increase of the value $K_V \cdot \Delta$ in all cases of different work materials. However, the manners of variation differ respectively. Fig.12 shows relations between the value $S \cdot D_\Delta$ and force components Ps, Qs and the force ratio ρ for five different work materials as for dressing condition while interference condition $K_V \cdot \Delta$ is constant. As can be seen in this figure, force components Ps, Qs decrease and the force ratio ρ increases with an increase of the value $S \cdot D_\Delta$. Higher value of $S \cdot D_\Delta$ results from coarser dressing and results in coarser distribution of cutting edges. For SUS304, the normal force Ps and the tangential force Qs increase rapidly with a decrease of the

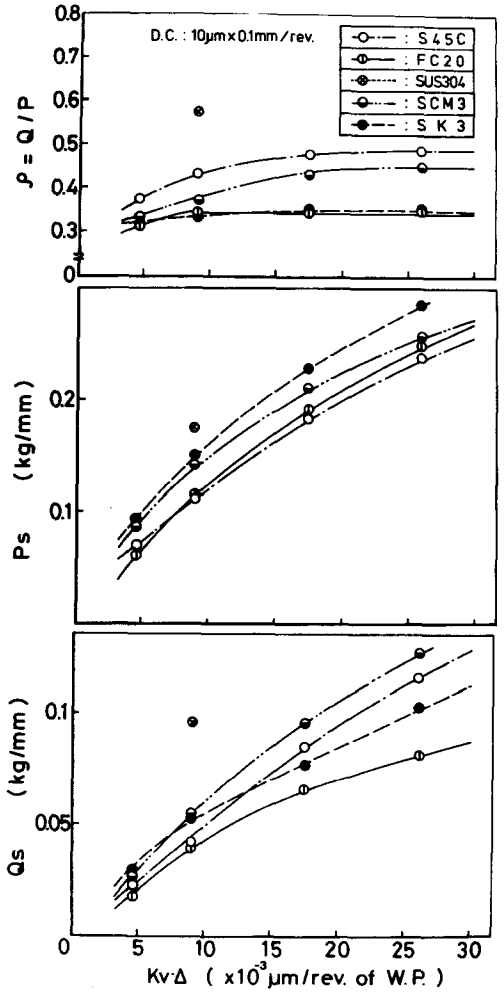

Fig.11 Relations between the Value $K_V \cdot \Delta$ and Force Components Ps, Qs and Force Ratio ρ

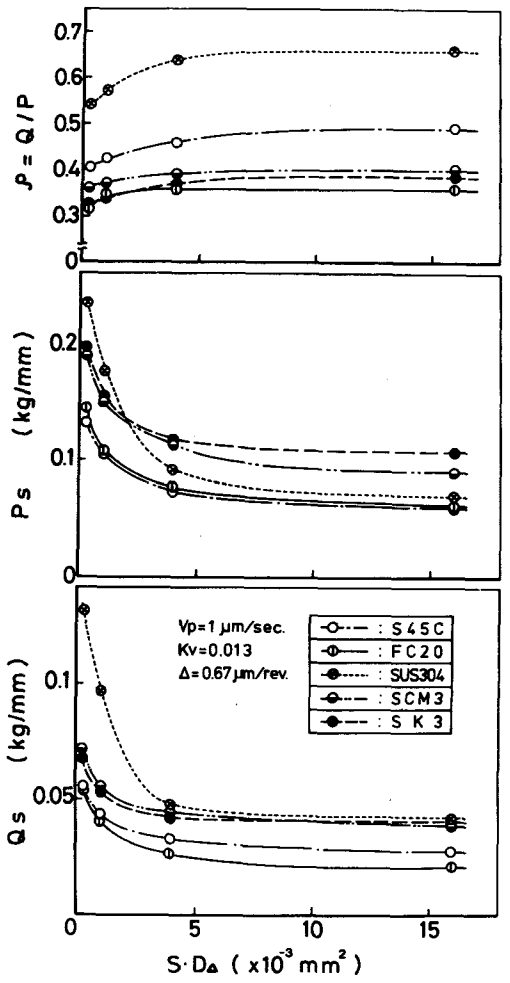

Fig.12 Relations between the Value $S \cdot D_\Delta$ and Force Components Ps, Qs and Force Ratio ρ

value $S \cdot D_\Delta$ as compared with other materials. This is due to high ductility and work hardening of SUS304, and loading of wheel occurs. From Figs.11 and 12, individual work materials show the same tendency of variation for the value $K_V \cdot \Delta$ or $S \cdot D_\Delta$, but the values differ respectively. This can be understood due to the difference of the chracteristics inherent to work materials.

5. Effect of Material Characteristics on Grinding Force

As mentioned in Section 4.3, grinding force may have a close relation to work material characteristics. In order to investigate this

relation, tension test and Charpy's impact test are carried out.

Fig.13 shows stress-strain curve of five materials and in Table 2 main material characteristic values are shown which are obtained from tension test and Charpy's impact test. Symbols used in this table are as follows;

σ_S : yield stress
σ_B : tensile strength
σ_T : breaking stress
φ : elongation
ψ : reduction in cross sectional area
E_B : breaking energy calculated from stress-strain curve
E_c : impact energy obtained from Charpy's impact test

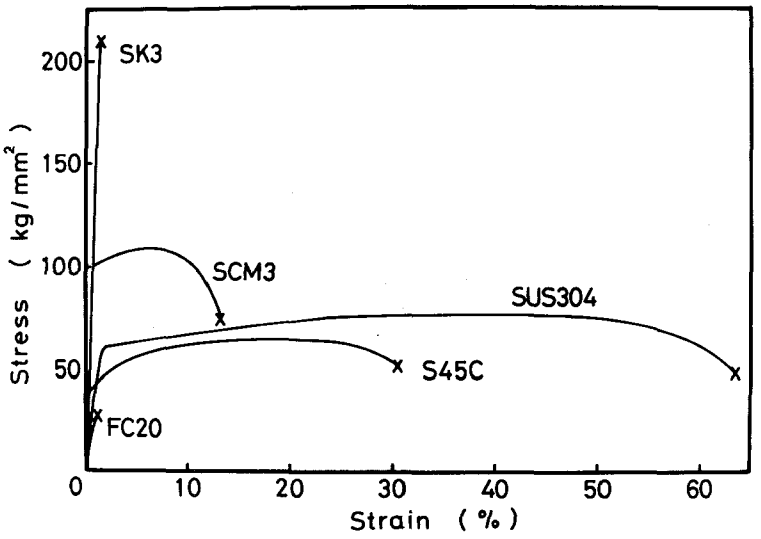

Fig.13 Stress-Strain Curve in Tension Test for Five Different Materials

Table 2 Material Characteristic Values

	σ_S Kg/mm²	σ_B Kg/mm²	σ_T Kg/mm²	φ %	ψ %	$\times 10^{-3} E_B$ kgm/mm³	E_c kgm/cm²
S45C	43	68	130.5	30	57.3	21.3	8.40
FC20	25	25	25.6	0.3	1.9	0.11	0.30
SUS304	60	75	107.3	64	57.5	42.7	24.89
SCM3	100	117	118.4	13	35.1	17.5	11.25
SK3	200	210	225.1	1.1	2.4	1.69	1.14

5.1 Relation between Material Characteristics and Normal Force

Fig.14 shows relations between micro-Vickers hardness H_V and the normal force Ps under four different dressing conditions. Micro-Vickers hardness is considered to have a close relation to grinding force in same material. As shown in this figure, however, the distinct relation is not be found between Ps and H_V.

Fig.15 shows relations between the yield stress σ_s and the normal force Ps under four different dressing conditions. As can be seen in this figure, Ps has a close relation to σ_s except for fine dressing conditions with SUS304. In case of SUS304, wheel loading occurs and normal grinding cannot be caccied out. It can be understood from the fact that the normal force is generated on pushing grains into workpiece.

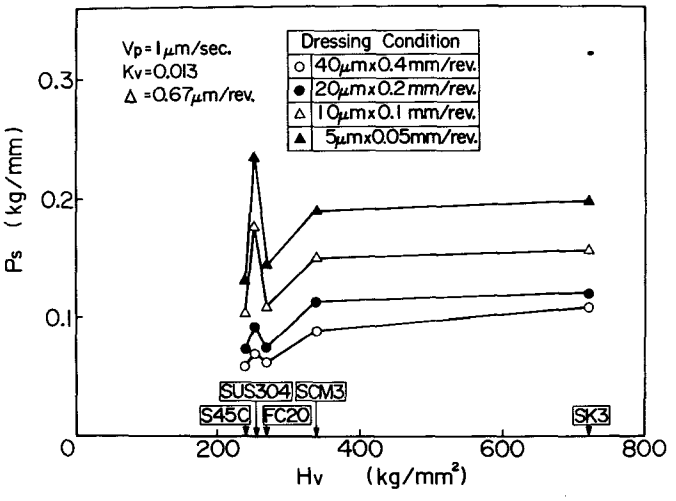

Fig.14
Relations between Micro-Vickers Hardness H_V and Normal Force P_S under Four Different Dressing Conditions

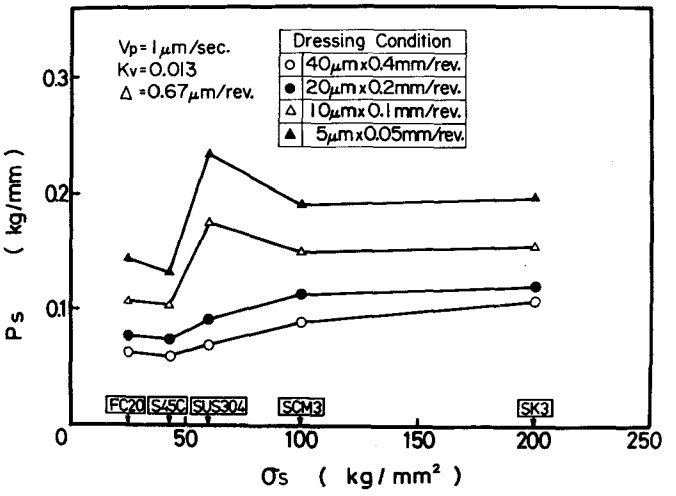

Fig.15
Relations between Yield Stress σ_s and Normal Force Ps under Four Different Dressing Conditions

5.2 Relation between Material Characteristics and Tangential Force

Tangential force of grinding is known to have a close relation to electric power of grinding machine. Then relation between the tangential force and the material characteristics related to energy is investigated.

Fig.16 shows relations between breaking energy E_B and the tangential force Qs under four different dressing conditions. As shown in this figure, it cannot be found the distinct relation between E_B and Qs. This may be due to large difference of strain rate between grinding test and tension test. Then relations between Charpy's impact energy Ec and the tangential force Qs are shown in Fig.17. The strain rate of impact test is larger than that of tension test. However, no apparent relation can be found from this figure.

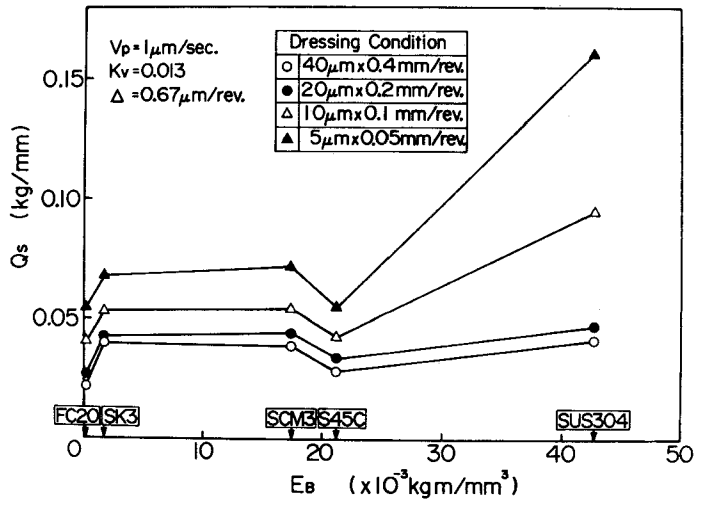

Fig.16 Relations between Breaking Energy E_B and Tangential Force Qs under Four Different Dressing Conditions

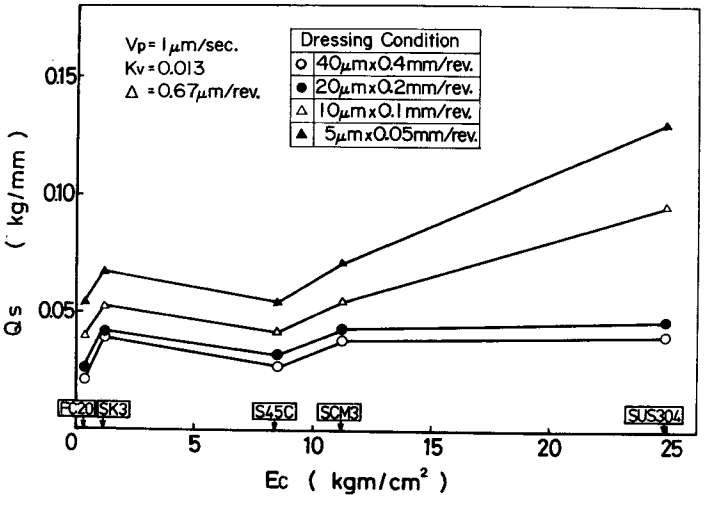

Fig.17 Relations between Impact Energy Ec and Tangential Force Qs under Four Different Dressing Conditions

5.3 Relation between Material Characteristics and Force Ratio

The force ratio ρ(=Q/P) in grinding is in general about 0.5. As shown before, however, this value varies with interference condition, cutting edge condition, workpiece condition.

Fig.18 shows relations between the force ratio ρ and Charpy's impact energy Ec under four different dressing conditions. No apparent relation cannot be found from this figure.

Fig.19 shows relations between the force ratio ρ and the elongation φ under four different dressing conditions. As can be seen in this figure, the force ratio ρ has a close relation to the elongation φ. That is, the direction of resultant force approaches to the grinding direction with an increase of ductility of material.

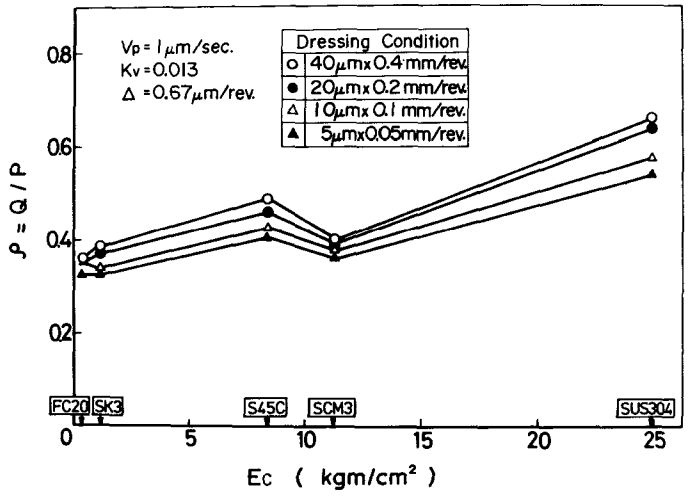

Fig.18 Relations between Impact Energy Ec and Force Ratio ρ under Four Different Dressing Conditions

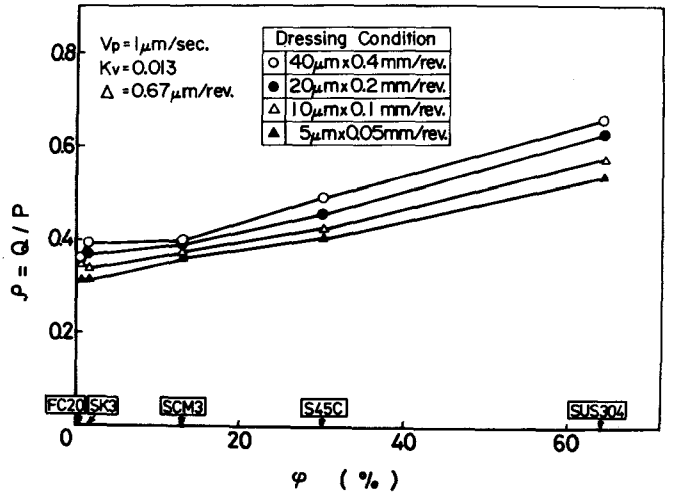

Fig.19 Relations between Elongation φ and Force Ratio ρ under Four Different Dressing Conditions

6. Conclusions

Grinding force is generated as a result of mutual interference between grinding wheel and workpiece, and it is very significant to make clear the force level and the direction for analysis of grinding phenomenon. In this paper, in order to analyze factors affecting grinding force components (normal force and tangential force) and the force ratio, relations between grinding force and interference condition, cutting edge condition and workpiece condition have experimentally been investigated. Main conclusions obtained in this paper are as follows;

(1) Normal grinding force, tangential grinding force and the force ratio are affected by the product of speed ratio and setting depth of cut as for interference condition.

(2) Grinding force components and the force ratio have a close relation to the product of square of dressing feed and cutting depth of dresser as for cutting edge condition.

(3) As for workpiece material condition, normal grinding force has a close relation to the yield stress and the force ratio is related to the elongation of workpiece material.

References

[1] K.OKAMURA and T.NAKAJIMA: Size Generation Process in Grinding, Proc. of the International Conference on Production Engineering, Tokyo (1974) 58.

[2] K.OKAMURA and T.NAKAJIMA: The Surface Generation Mechanics in the Transitional Cutting Process, Proc. of the International Grinding Conference, Pittsburgh, Pa. (1972) 305.

[3] K.OKAMURA, T.NAKAJIMA and Y.UNO: Analytical Description of Accumulation Phenomenon in Grinding, Annals of the CIRP, 24, 1 (1975) 243.

[4] K.OKAMURA and T.NAKAJIMA: Fundamental Analysis of Grinding Process, SME Technical Paper, MR70-183 (1970).

[5] K.OKAMURA, T.NAKAJIMA and K.WATANABE: Contact Stiffness Theory in Grinding (3rd Report), Journal of the Japan Society of Precision Engineering, 36, 4 (1970) 241.

[6] K.OKAMURA, T.NAKAJIMA, M.UEDA and T.UCHIDA: Study on the Cutting Mechanism of Abrasive Grain (1st Report), Journal of the Japan Society of Precision Engineering, 32, 4 (1966) 287.